3rd Specialty Conference on Material Engineering & Applied Mechanics
3e Conférence spécialisée sur le génie des matériaux et mécanique appliquée

Montréal, Québec
May 29 to June 1, 2013 / *29 mai au 1 juin 2013*

Characterization of concrete fracture properties using digital image correlation technique

W. Polies, F. Ghrib, S. Cheng,
Department of Civil and Environmental Engineering, University of Windsor

Abstract: One of the most critical demands in the industrialized world lies in the assessment of the integrity of existing infrastructures and the monitoring of their safety. Accurate assessment methods allow engineers to improve maintenance and repair strategies of structures based on reliable and objective data. Techniques based on non-contact, non-disturbing methods proved to be valuable for generating accurate structural measurements. In particular, the monitoring of the concrete fracture is of the most importance. In this research paper, the Digital Image Correlation (DIC) is employed to characterise the development of the fracture process using the wedge splitting test. The experimental observations are thoroughly discussed; with special attention being placed on the monitoring of the crack path, the size of the fracture process zone, the traction free zone (crack extension), the variation of dissipated energy and tensile damage along the crack path.

1 Introduction

Concrete is a quasi-brittle material; when cracked its behaviour is characterized by the presence of a fracture process zone (FPZ), where the material undergoes softening damage, ahead of the crack tip. The characterisation of the fracture process is essential for studying the stability of concrete structures. Traditional techniques used for identifying concrete fracture properties are based on the overall specimen response and the crack opening displacement is measured by means of a clip-gauge. This technique can only measure global responses and no local information can be extracted. Alternatively, non-contact measurement techniques have been used; but suffer from low measurement accuracy, laborious post-processing, or high sensitivity to environmental temperature, air draft, or vibrations from testing machines. The demand for non-contact and non-disturbed deformation measurements has led to the development of a new technique based on optical measurement that is capable of monitoring the FPZ and crack evolution in addition to providing an accurate measurement of the crack opening displacement (COD) from a single test.

Various experimental techniques for measuring the FPZ have been described including the use of: scanning electronic microscope (Mindess and Diamond, 1982 and Krstulovic-Opara, 1993), surface holographic measurements (Jacquot and Rastogi, 1983 and Raiss et al., 1990), dye penetration (Swartz and Go, 1984 and Swartz and Refai, 1989), acoustic emission (Maji and Shah, 1988 and Mihashi et al., 1991), laser holographic interferometry (Castro-Montero et al., 1990), laser speckle technique (Horii and Ichinomiya, 1990), vacuum impregnation technique (Mier, 1991), digital image cross-correlation (Choi and Shah, 1997), CAT scan (Landis and Nagy, 1998), X-rays (Otsuka and Date, 2000), optical fiber technology (Rossi and Le Maou, 1989, Leung et al., 1998, Denarie et al., 2001, and Hadjab et al., 2004), scanning computer vision (John and Shah, 2002), and CT-scan (Schlangen, 2008). These methods vary in their ability to provide detailed measures of the FPZ and crack profile under various conditions. For example, in addition to the measurement of the FPZ, the crack profile was obtained by the impregnation technique. Due to its destructivity nature, impregnation technique cannot provide information about crack

evolution during loading (Jan and Stang, 2010). On the other hand, the approximate crack tip position determined by acoustic emission, which provides an estimation of the dissipated energy, failed to characterize the crack profile. Although optical fiber technology using fiber bragg grating successfully detected the FPZ, a major drawback was that the fibers are very sensitive to environmental temperatures, vibrations and air draft (Denarie et al., 2001). Furthermore, strain measurements obtained with this technique could be unreliable because of the fiber damage or the presence of an adjacent aggregate shielding the material from strains. Consequently, the position of the optical fiber needs to be specified before the test when more than one gauge should be installed, as some of them may be positioned outside of the actual FPZ.

To the best of the authors' knowledge, most of the investigations dealing with the characterization of the FPZ along the specimen's length focused on the global fracture behaviour. Very few investigations studied the variation of concrete properties, such as crack opening or dissipated energy along the crack path during various loading stages in a single test. Concrete fracture pattern is naturally not a smooth process because of the material internal heterogeneity; gauges attached to the specimen cannot provide accurate data. Therefore, the need for a precise non-contact and non-disturbing technique that is capable of monitoring the FPZ is recognised by many researchers. The main objective of this research is to illustrate the use of such technology to estimate the variation of the dissipated energy and the tensile damage along the crack path, and monitoring of the crack propagation process.

Optical techniques have proven to be valuable for characterizing the properties of advanced materials, especially those exhibiting inhomogeneity. For example, Digital Image Correlation (DIC) is an optical technique used to visualize surface deformations based on the processing of data encapsulated in digital images. DIC is a non-disturbing and non-contact measurement technique of displacement and strain on visible surfaces. When DIC is used for the assessment of concrete fracture, it is possible to monitor the development of the FPZ without interference and with marginal effect of the testing machine vibrations. Image recognition is used to analyze and compare digital images obtained from the surface of a substrate. This technique is not restricted to a single axis or to specific points on the surface, so it is capable of providing a large set of data of the entire surface of the specimen. For all of the aforementioned reasons, and the ability to obtain undisturbed data during the failure process as well as data from any point on the specimen's surface, the DIC technique was chosen to generate the load-crack opening displacement (P_{sp}-COD) relationship from the analysis of digital images obtained while monitoring the FPZ during loading.

In this research work, the characteristics of the FPZ associated to mode I fracture behaviour of plain concrete is studied using the wedge splitting test (WST). The tests were carried out in an electro-hydraulic closed-loop INSTRON testing machine. The principal parameters are the applied vertical load, and the COD obtained by clip-gauge and DIC.

2 Experimental Investigation of the WST using DIC

DIC is an optical based technique for capturing surface deformations by post-processing digital images of the specimen's surface during testing. Peters and Ransom (1982) were the first to introduce this technique in the early 1980's. Currently, DIC is widely used to examine the deformation of engineering materials, including concrete and related cement-based materials (Choi and Shah, 1997; and Lawler et al., 2001). Modern DIC systems use two stereo cameras with different viewing angles, to measure 3D displacement fields.

The DIC technique is based on inferring the displacement of the material being tested, by tracking the deformation of a random speckle pattern on the specimen's surface. Mathematically, this is accomplished by finding a region in the image associated to a deformed configuration that maximizes a normalized cross-correlation score with a small subset of the reference image that was taken while no load was applied. By repeating this process for a large number of subsets, full-field deformation data can be obtained. Macro-image facets, which represent virtual gauges, are areas created throughout the image using sets of pixels (typically 5-20 pixels per side) distributed across the image, thus allowing sub-pixel

accuracy (Tyson, 2001). The number of facets within an image depends on the cameras' resolution, as well as the defined size and overlap of the facets; however, it is possible to define thousands of facets across an image. A 13 x 13 pixel facet with a 2 pixel overlap allows for the formation of over 10,000 facets on an image with a resolution of 1280 x 1024. The ideal facet should contain several discrete pixels, the centre of each of these facets provides surface coordinates, and the locations of these facets are tracked through a series of images called 'stages'. When a specimen is loaded, its surface image deforms in response to the loading, and at each stage the displacement values can be obtained in relation to a reference stage. Typically, the initial image at zero loading is taken as the reference frame from which the reference measurements are taken. The accuracy of DIC results depends on many factors, including the resolution and configuration of the used cameras, the quality of the light source, the accuracy of the calibration step, and the quality of the surface pattern. In addition, the displacement sensitivity increases when increasing the field of view. High sensitivity can be obtained, with a displacement sensitivity on the order of 1/30,000 of the field of view (Tyson, 2001), and a strain sensitivity between 50 and 100 Microstrain.

For this research study, an approach to the evaluation of fracture tests based on DIC was conducted using the commercial ARAMIS system. The images of the specimen cover the entire area around the expected crack tip. DIC is not restricted to a single axis measurement or to specific points as is the case with most gauge-based measurement techniques. Consequently, the displacement and strain can be measured at any point on the surface after the test. The crack evolution can be tracked and the variation of the crack opening displacement and the dissipated energy along the crack path can be determined directly from the analysis of the recorded images during different loading stages.

2.1 Investigation of the Crack Evolution and Development of the FPZ

It is well established that prior to any loading, concrete contains naturally distributed internal defects. Concrete cracking process is characterised by three stages (i) stable micro-cracking (ii) unstable micro-cracking and (iii) bridging phase (Shah et al. 1995). The micro-cracking region in front of the traction-free crack tip in concrete is referred to as the FPZ (Hillerborg et al., 1976) and the overall fracture behaviour of concrete is influenced by this zone. As realized by Shah and McGarry (1971), Linear Elastic Fracture Mechanics (LEFM), where the size of the FPZ vanishes, cannot be directly applied to geomaterials including concrete and ceramics due to the presence the crack-bridging stress phenomenon. Other difficulties for using fracture mechanics to describe concrete performance include: the tortuous crack path, the difficulty of determining the location of the crack tip in concrete due to aggregate bridging, and the FPZ size that is closely related to the fracture energy, G_F (Wittmann and XZ, 1991). It is now recognised that the fracture energy is the most important concrete fracture properties which represents the energy required to propagate a crack by one unit area. Consequently, in addition to the crack tip opening displacement (CTOD), an accurate description of concrete fracture should include other features such as: the tortuous crack path, the position of the crack tip, the dissipated energy along the crack path, and the size of the FPZ.

The experimental identification of the FPZ in geomaterials and concrete in particular requires the deformation measurements at the crack tip during the fracture process. This task is difficult because it requires the measurements of the localized deformation around the crack tip that cannot be obtained accurately by conventional gauges. In the present paper, we propose to exploit the capabilities of DIC in measuring local displacement around the crack tip to study the development of the FPZ. DIC makes it possible to study the dynamics of crack propagation and energy dissipation during the fracture process. Attention was also paid to the changes in the crack tip position associated with the evolution of the crack path, toughening mechanisms in the FPZ, and variation in the energy dissipated along the crack path.

The identification of the fracture parameters requires the measurements of the load and crack opening displacement (COD) at the crack tip. The Wedge Splitting Test (WST) was chosen to illustrate the usage of the DIC procedure to determine the FPZ length and the measurement of the COD along the crack path. The necessary measurements were obtained by post-processing the specimen images. Once the crack path was revealed parallel sections were defined along the crack path and used to compute the

displacement discontinuity along the crack. The COD along the crack path was obtained by computing the length change of the parallel sections corresponding to each loading stage in comparison to the reference stage of zero loading.

The crack opening displacement along the crack path (COD) for various loading stages were determined first. Due to the limitation of the calibration panel, which controls the size of the cameras field of view, the area limited within 50 mm of the original crack/notch tip is studied. During the post-peak phase, the load-COD curve revealed two zones, i.e. the stable and unstable stages. The stable stage ended at approximately 37.2% of the peak-load, and the second zone started at 21.6% of the peak-load (after the initiation of a traction-free zone). This observation leads to suggest the validity of using the simple bilinear softening model (Roelfstra and Wittmann, 1986; Guinea et al., 1994; Sousa and Gettu, 2003; RILEM, 2007) to estimate the strain softening behaviour of concrete in the FPZ. The popularity of the bilinear model's approximation of the tension softening diagram stems from the fact that the model captures the impact of two major mechanisms responsible for the tension softening observed in concrete. The initial, steep branch of the tension softening diagram is a stable cracking stage resulting from micro-cracking within the matrix, whereas the second stage can be associated to fracture at aggregate-matrix interface (Abdalla and Karihaloo, 2004).

Accurate assessment of the length of the FPZ is essential for predicting failure of concrete members and for selecting the appropriate dimensions of the test specimens (Li and Marasteanu, 2010). As noted earlier, one of the difficulties encountered when investigating the development of the FPZ in concrete, including its length, is the precise determination of the crack tip's position due to the impact of aggregate bridging and variation of the crack path across the structure's depth. For this study, however, both the position of the fictitious crack tip and the length of the FPZ at each loading stage were defined at the point where the crack opening is zero; in other words, the effect of micro-cracks in front of the newly formed fictitious crack tip was ignored when the FPZ length was estimated.

The FPZ was evaluated at the eleven loading stages shown in Figure 1 referred from (a) to (k). Figure 2, shows the development of the FPZ during some of these stages. At 2.0 kN (22% of the peak load) (Figure 2 (a)), the FPZ length was 2 mm (i.e., 1.5% of the ligament length). The CTOD was 0.0004 mm and micro-cracks were distributed across the whole field of view.

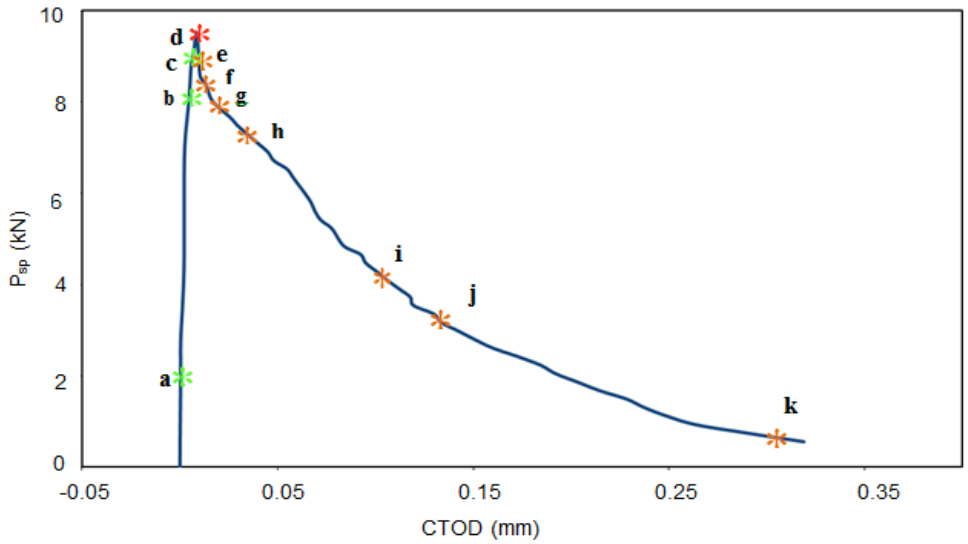

Figure 1: Splitting load-Crack tip opening displacement (P_{sp}-CTOD) relationship associated with different cracking stages in the WST-specimen (WST2), and assessed using DIC.

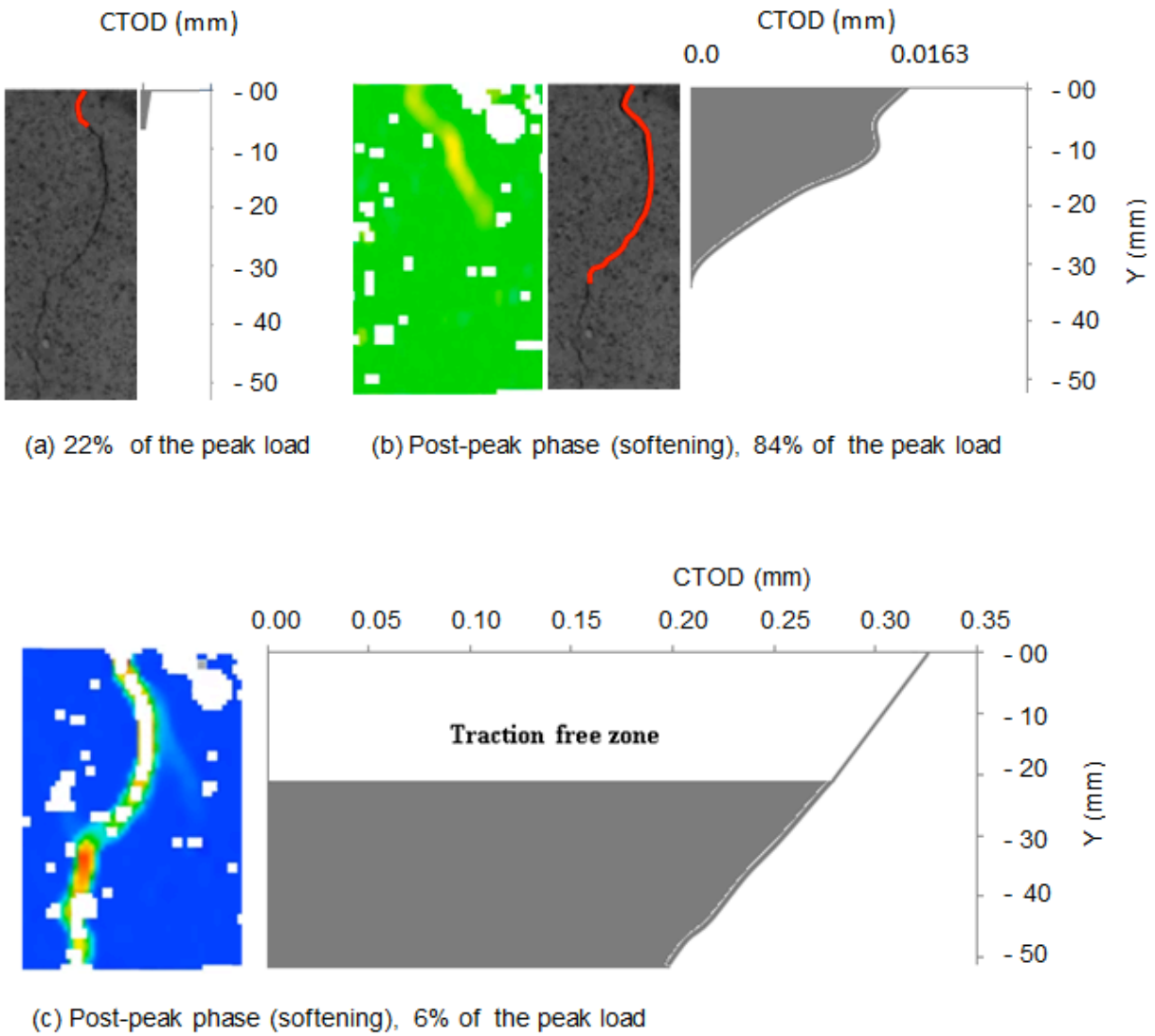

Figure 2: Development of the FPZ and the traction free zone during loading phases; (a) point a on Fig.1, (b) point g on Fig. 1, (c) point k on Fig. 1.

The variations in the length of the FPZ associated with the splitting load are summarized in Table 1 and Figure 3. Although the length of this zone increased with the loading, the rate of this increase was higher from stable cracking stage (96% peak load) to unstable cracking stahestage (d) (100% peak load), shown in Figure 1, followed by slow growth within the post-peak phase. However, the growth of the FPZ length in the post-peak start to increase again with the initiation of the traction free zone at 84% of the splitting load (Table 1). Further development of the FPZ could not be monitored, since the FPZ extended beyond the field of view.

More details about the development of the traction free zone during the post-peak phase is provided in Table 2 and illustrated in Figure 4. The traction free zone initially grew slowly (from 2 to 8 mm; an increase of 6 mm) as the post-peak P_{sp} decreased sharply from 25.49 % to 9.8% of peak load, a change of over 16%. The length of the traction free zone grew another 6 mm as the load decreased from 9.8% to 7.84%, a change of less than 2%. At this point, the size of the traction free zone continued to grow despite little change in the post-peak P_{sp}, which is maintained at 5% level while the traction free zone extended an additional 38 mm to reach a total length of 52 mm.

Table 1: Variation of the FPZ length with splitting load

Points on Fig. 1	splitting load P_{sp}%	FPZ length L_{FPZ} (mm)	L_{FPZ} /L_{lig} %
	0	0	0
a	22	2	2
b	84	6	5
c	96	12	9
d	100	28	21
e	90	30	23
f	88	31	24
g	84	36	28

Table 2: Development of the traction free zone

Traction Free Zone (mm)	Post-peak P_{sp}%
2	25.49
7	16.00
8	11.76
8	9.80
14	7.84
21	5.88
23	4.51
25	4.29
31	4.25
52	4.22

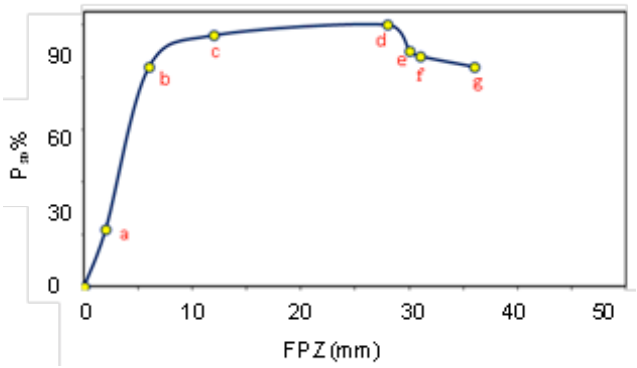

Figure 3: Variation of the FPZ length with the splitting load ($P_{sp;}$ % of peak load)

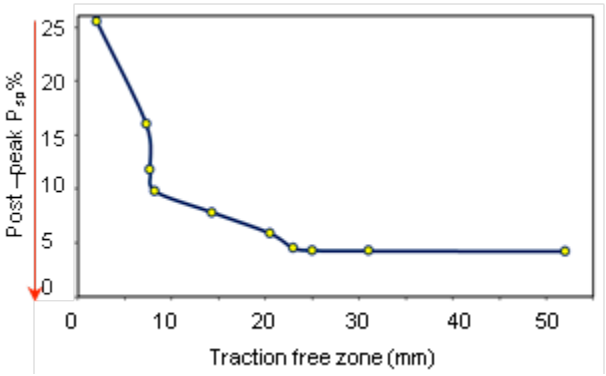

Figure 4: Growth of the traction free zone during the post-peak phase (softening phase)

2.2 Energy Dissipation and tensile damage along the Crack Path

The amount of energy required dissipated in the cracking process along the crack path was derived from direct measurement COD using DIC without resorting to inverse analysis. To calculate the dissipated energy, the P_{sp}-COD curves for various locations along the crack path are required. The COD was determined for a series of sections along the crack path at each loading stage, and used to calculate the dissipated energy at various distances, *y*, from the crack/notch tip.

The energy required to propagate the crack along the crack path that is a specific distance, *y*, from the crack/notch tip, is shown in Figure 5. The fracture energy was calculated by dividing the area under the *P_{sp}-COD* curve obtained at each location, *y*, during the post-peak phase by the fracture area. Note that in the current study, this finding is limited to the amount of energy dissipated at locations that are within 50 mm from the crack/notch tip, this distance is controlled by the size of the cameras' field of view.

The dissipated energy is influenced by the size of the FPZ, which changes during the loading process. It was observed from the images that the width of the damaged zone (FPZ) increases with the loading up to the peak-load is reached. During the post-peak phase, the width of the FPZ starts decreasing and then remains constant as the crack runs along the ligament. This means that the dissipated energy is not equally distributed along the ligament; this observation is evident in Figure 5. From the calculated fracture energy, one can calculate the tensile damage in the specimen D= g/Gf. Figure 6 shows the variation in of

the tensile damage along the crack path. It is clear that the use of DIC allows the estimation of the crack bridging reserve with along the cracking process (Duan et al., 2002).

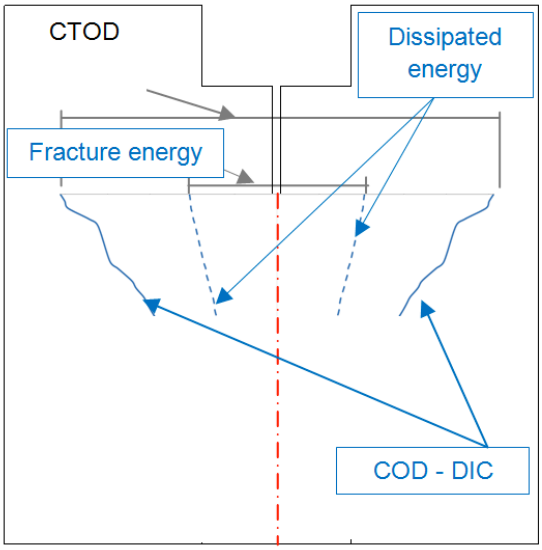

Figure 5: The dissipated energy and COD along the crack path on the WST-specimen

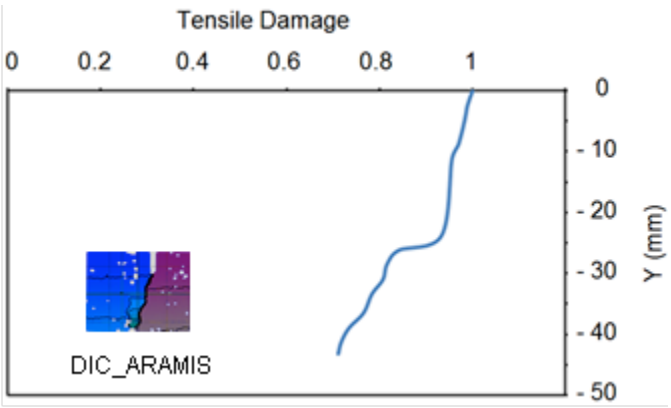

Figure 6: The tensile damage along the crack path assessed using digital image correlation (DIC)

2.3 Assessment of the Development of the FPZ using the DIC Technique

Under loading concrete structures, the high-stress state near the crack tip induces micro-cracking defects and initiates fracture. Mindess and Diamond (1982) studied the crack tip in concrete using a scanning electron microscope; they reported that concrete crack surface was tortuous a cracking could produce rough dislocated surfaces. During the present work, we have paid particular attention to the development of cracking process, in particular, the measurement of the strain developed in the FPZ using the DIC technique.

A new WST-specimen was chosen to study the development of the FPZ. Figure 7 (a) depicts the strain distribution at 34% of the peak load (Point A in Figure 1). As it can be seen, the initiation of internal cracks was detected at this stage; micro-cracks were concentrated at the crack tip, and are represented by a light spot indicating the FPZ. The recorded load, P_{sp} , was 5.6 kN and the CTOD was 0.006 mm. At loading stages prior to Point (A), representing elastic stage, the specimen behaves elastically with negligible distributed tensile strain at the crack tip. This observation is consistent with observations made by Shah et al. (1995) using acoustic emission based measurements, which indicated that the initiation of internal cracks is negligible before the proportional limit is reached. As the load increased beyond Point A (Figure 8), more internal cracks were detected and the area around the crack tip started to exhibit changes; however, this was accompanied by a slight increase in tensile strain and CTOD. When this new cracking stage started, the isolated internal cracks continued to spread randomly over the specimen without any particular localization.

A new cracking stage was detected when 82% of the peak-load was applied, as shown in Figure 7(b); the load at this stage, Point B in Figure 8, was 13.4 kN and the CTOD was 0.019 mm. A new cracking stage was characterized by the appearance of a narrow band of internal cracks indicating that the damage had started to localize in to a band of microcracks. This band continued to propagate in a stable manner until the peak-load was applied. As loading slightly increases, more internal cracks become appearent,

particularly in the area around the band and at the crack tip and the length of the band of microcracks continued increasing and became more clearly defined, indicating that the major crack was propagating. This phenomenon is observed by the increased strain within the band only. Based on the distribution of the microcracks and the strain across the specimen's surface, the length of the FPZ was estimated to be approximately 20 mm at 94% of the peak-load. When the applied load, P_{sp}, was increased to approximately 96% of the peak-load, the CTOD measured to be 0.027 mm. At this point, the length of the FPZ was approximately 22 mm, and its width was 30 mm. Increasing P_{sp} to about 99% of the peak load, led to the appearance of a new micro-crack band on the right side of the WS-specimen's surface. With increased loading, the strain within this new band increased also, and the band became clearly defined. However, this phenomenon was accompanied by decreasing strain within the first band of micro-cracks, indicating the closure of these micro-cracks. At this point (P_{sp} = 99% of peak load), the length of the FPZ was approximately 23 mm and its width was 28 mm, while the CTOD was 0.031 mm with 0.005 maximum strain at the crack tip(Fig. 7b).

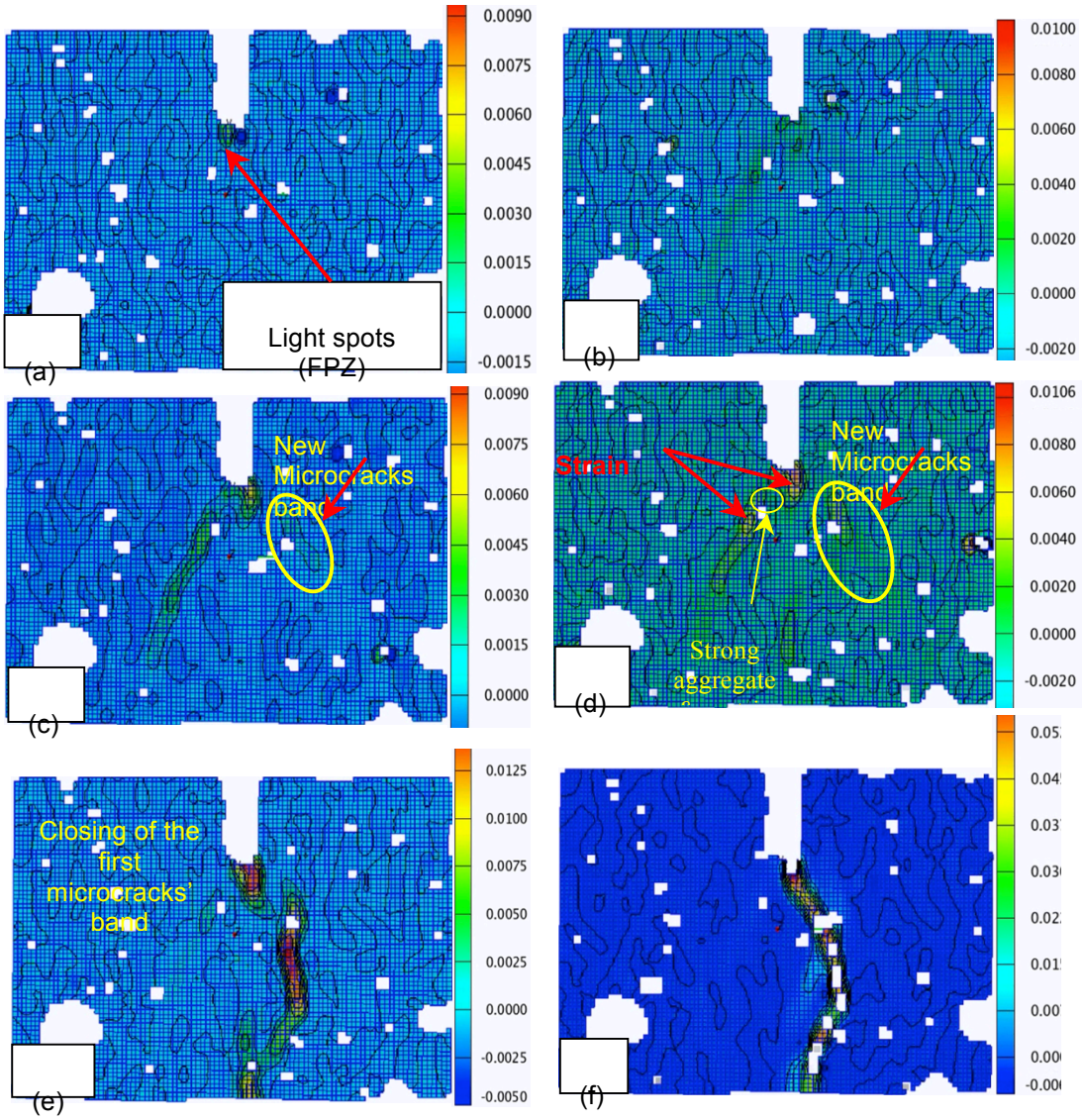

Figure 7: Strain distribution over the WST-specimen's surface assessed using DIC; (a) 34% of the peak load- Point A in Fig. 8, (b) 99% of peak load- Point B in Fig. 8, (c) at the peak load-Point C in Fig. 8, (d) 99% of the peak load-post peak stage, (e) 86% of the peak load-post- peak stage, (f) 21% of the peak-load post- peak stage.

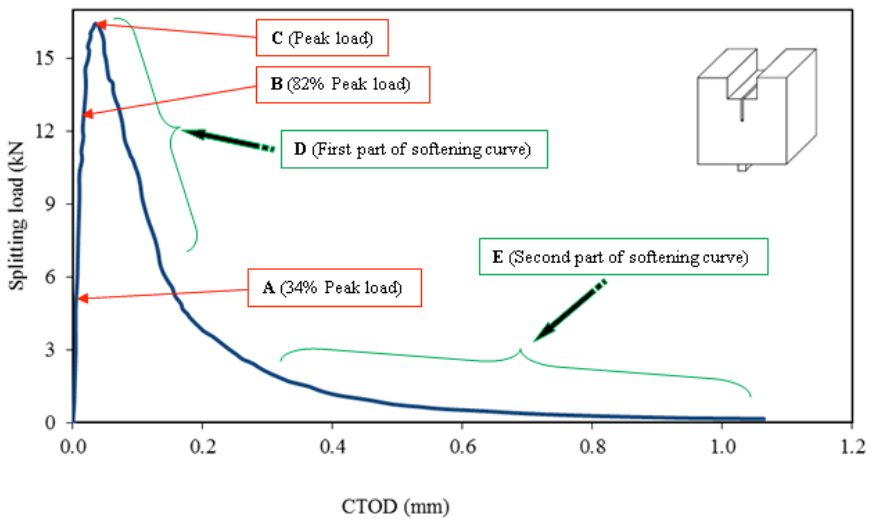

Figure 8: Splitting P_{sp}-CTOD associated with different cracking stages

Figure 7 (c) illustrates the strain field measurements obtained for the peak-load of 16.4 kN represented by Point C in Figure 8. The maximum recorded strain was 0.006 at the crack tip, and the CTOD was 0.034 mm. Since the application of the peak-load was followed by the critical propagation of the major crack (softening stage), this CTOD represents the critical crack tip opening displacement ($CTOD_c$). At this stage, the width of the FPZ continued decreasing which may be associated with unloading of the material located farther away from the crack path. This phenomenon indicates that the softening stage was initiated without the occurrence of sudden failure because of the cohesion effect within the FPZ. When the peak-load was applied, the length of the FPZ was approximately 28 mm (21.5% of the ligament length); this increase in length was accompanied by a decrease in the width of the FPZ to approximately 22 mm.

After the peak-load the strain in the FPZ increased and a crack branching in the form of new crack band appeared Figure 7(d). With a slight loading increase, the new band of microcracks started to localize, indicating the appearance of a new crack at the loacation. This phenomenon can happen when the main band (i.e., first band of micro-cracks) reaches an aggregate. Moreover, the observed damage consisted of a major crack opening within the crack band associated with the unloaded region of the specimen outside of this band. This phenomenon was accompanied with a narrower FPZ width, as well as increase of the strain within the new crack band. The length of the FPZ continued to increase after the peak load; however, it was not possible to estimate its length, as the FPZ extended beyond the 50-mm field of view calibrated for the DIC system's cameras in this study.

The CTOD continued to increase during the post-peak phase, while the width of the band of microcracks near the crack/notch tip decreased, indicating the initiation of a traction-free region where the initial crack started to expand (Figure 7 (e)). Accordingly, the width of the FPZ continued to decrease, and the strain at the new crack path continued to increase while the strain at the original band of micro-cracks decreased. The final unstable cracking stage, illustrated on the softening curve by stage E (Figure 8), is characterised by the crack bridging stresses resisting the applied load. The test was stopped at a load level of 0.15 kN, and the CTOD at this point was 1.064 mm. During this final stage, the change in the CTOD was constant, and the specimen was subjected to a compressive stress away from the opened crack.

At the end of the test, the crack was not fully opened although it appeared on the surface images as fully developed crack. This observation could indicate that a crack formed on the specimen surface is not fully developed within its depth. Accordingly, the WS-specimen may continue to sustain tensile stress that is characterized by the material's tensile stress-separation relationship; consequently, additional energy is needed to fully open the crack.

3. Conclusion

The optical non-contact DIC measurement technique is proved to be valuable for characterizing concrete fracture properties. This study demonstrates the use of the DIC technique to generate the P_{sp}-*COD* softening curve along the crack path whereas classical measurement method using clip gauge can provide the global structural response of the specimen. The study also demonstrates the utility of this novel technique for the investigation of crack evolution and the development of the FPZ zone.

The following conclusions were successfully documented:

- The variation of the dissipated energy and the crack opening displacement along the crack path can be estimated using DIC, while only global measurements can be obtained by traditional clip-gauge technique.
- The experimental observations revealed that the development of the FPZ is slow in the pre-peak load stage, and then it increases suddenly, this increase rate continues within the stable cracking phase. In the post-peak range a slow growth of the FPZ size is reported. These observations lead to suggest that the pre-peak load is a critical stage in the loading history.
- The FPZ width increases with the loading, and reaches its maximum width with the initiation of the localization of micro-cracks (at about 96% of the peak load when the length of the FPZ starts to increase rapidly). The maximum width of the FPZ is approximately three times the maximum aggregate size. In the post-peak phase, the width of the FPZ continued to decrease and then stabilises as the crack ran along the ligament.
- The DIC measurement technique allowed us to identify the distribution of the dissipated energy along the crack path. A damage index was also defined to illustrate the strength reserve during the crack propagation.

The DIC technique met the experimental requirements for the WST and made it possible to study the dynamics of crack propagation by monitoring the evolution of the tortuous crack and energy dissipation during the fracture and avoiding the limitations of traditional measurement techniques. Consequently, the use of DIC is recommended for the study of the fracture behaviour of concrete structures, and can be used for both assessment and monitoring purposes.

5. REFERENCES

Choi S., Shah SP. 1(997)., Measurement of deformations on concrete subjected to compression using image correlation. Exp Mech;37(3):307–13.

Hillerborg, A., Modéera, M., and Petersson, P. (1976). Analysis of crack formation and crack growth in concrete by means of fracture mechanics and finite elements. *Cement and Concrete Research*, 6(6), 773-782.

Opara K. (1993). Fracture process zone presence and behaviour on mortar specimen. ACE Materials Journal, Bol. 90,No. 6, 1993, pp. 613-626.

Optical Measuring Techniques (GOM) mbH. (2005). ARAMIS user manual.

Orteu, J. J., Cutard, T., Garcia, D., Cailleux, E., & Robert, L. (2007). Application of stereovision to the mechanical characterisation of ceramic refractories reinforced with metallic fibres. *Strain*, 43(2), 96–108.

Otsuka K. & Date H. (2000). Fracture process zone in concrte tension specimen, Engineering Fracture Mechanics, 65(2-3), 111-131.

Maji & Shah (1988). Process zone and axoustic-emission measurements in concrete. Journal of Experimental Mechanics, 28(1), 27-33.

Østergaard, L., Lange, D., & Stang, H. (2004). Early-age stress–crack opening relationships for high performance concrete. *Cement and Concrete Composites*, 26(5), 563-572.

RILEM (The International Union of Testing and Research Laboratories for Materials and Structures), edited by: Shah, S. P., & Carpinteri, A. 1989. *Fracture mechanics test methods for concrete* (Technical Committee 89-FMT) Chapman and hall.

Shah, Swartz, and Ouyang (1995). Fracture Mechanics of Concrete. John Wiley & Sons, Inc. USA.

Wittmann FH, Hu XZ. (1991). Fracture process zone in cementitious materials. Int J Fract;51(1):3–18.